

Article

Design and Fabrication of Low-Speed Wind Tunnel (LSWT)

Umair Asghar, Muhammad Anas Wazir *, Muhammad Kaleem Wazir, Abbas Khan, Muhammad Usama, and Osama Subhan

Department of Mechanical Engineering, University of Engineering and Technology, Peshawar, Pakistan

* Correspondence: Muhammad Anas Wazir (19pwmec4713@uetpeshawar.edu.pk)

Abstract: The design and fabrication of a low-speed wind tunnel (LSWT), which is a critical component for testing and comprehending aircraft aerodynamics, is presented in this study. Despite the increasing prominence of computational fluid dynamics (CFDs) in manufacturing engineering, wind tunnels remain essential for the intricate development of aircraft and automobile designs with complex flow interactions. Using SolidWorks, we focused on controlling flow turbulence approaching the test section, emphasizing performance and quality parameters. The construction of the wind tunnel used plywood with an axial fan regulating the airspeed, and Arduino facilitated data acquisition. The drag and lift on the Y Clerk Airfoil were quantified by two load cells along the XY-axis, complemented by a Pitot Static Tube and a multitube inclined plane manometer for pressure and velocity calculation. Fusion 360 simulation software was used to analyze pressure and velocity profiles at speeds ranging from 10 to 20 m/s, providing a comprehensive quantitative evaluation of the wind tunnel's capabilities. By emphasizing both design innovation and quantitative performance metrics, this study underscores the continuing significance of wind tunnels in engineering.

Keywords: Airfoil, CFD Analysis, Low-speed Wind Tunnel, Pressure Profile, Velocity Profile

1. Introduction

Wind tunnels are the most important tool used to find the aerodynamics of different objects. One can understand the importance of Wind Tunnels in the Design and Manufacturing field from the fact that even in the 21st century when Computational Fluid Dynamics (CFD) is making progress rapidly, wind tunnels have their place; they are still important for designing different complex geometries [1]. One way to make anything seem like it's flying through the air or moving over the ground is to put it in a wind tunnel, which is just a big tube with air flowing through it. We are surrounded by fluid everywhere, and we are interested in controlling the fluid flow around us or the bodies that interact with the flow in a complicated way. Engineers have used this technology to build high-precision, high-performance engineering applications. Ships, boats, aircraft, rockets, and automobiles are just a few examples of aerodynamics [2]. The primary purpose of wind tunnels is to investigate the effects of wind on bodies by simulating wind flow around them and determining the pressure exerted on models [3]. A smoke machine is often used in wind tunnels that use generators to visualize airflow patterns and turbulence. Designers and researchers need these tools. This portion (the test section) gained prominence as a result of the impact on the characteristics of flow inside the experiment section. Also, it is in charge of the most crucial aerodynamics testing device's performance accuracy.

Maurya. et al. [4] designed and built a low wind tunnel to reduce drag and lift forces. They found that as height increases, velocity increases, and pressure reduces on the

solid object, and that after maximum height, velocity declines and pressure increases. Kareem et al. [5] performed an aerodynamic analysis of a low-speed wind tunnel with the main goal of improving airflow parameters by modifying the contraction section. After looking at a lot of different profiles, they settled on the 9th-order wall profile with a length of 0.93 L and an inflection point of 0.65 L for the ideal tunnel contraction. An open-circuit subsonic wind tunnel was designed and built by Patil. et al. [6] to study the influence of wind on various structural element prototypes. They conducted analyses of both cylindrical and wing objects and concluded that shape, size, and material selection were important factors in their analysis and construction of a wind tunnel. Siregar and Umurani [7] fabricated an open-style low-speed wind tunnel for educational objectives. After conducting tests with airfoils, wings, and drag coefficients and analyzing the data, they concluded that their wind tunnel was also appropriate for aerodynamic research and instruction. In a low-speed open return wind tunnel, Farnsworth et al. [8] designed and tested a longitudinal gust generator. They quickly changed the blockage ratio at the inlet for low test section flow speed using hindering flow-hindering louvers. They created a mathematical model to represent the behavior of the wind tunnel precisely, and they concluded that it could accelerate longitudinal velocity at huge amplitudes.

The main goal of our project was to achieve laminar fluid motion inside the test section of a wind tunnel, for which we used different sections, i.e., Contraction chamber, diffuser, and settling chamber [9]. The main role of the contraction

chamber is to increase the mean velocity, which results in low air pressure and more energy-efficient wind tunnel operation [10]. We also want fewer pressure losses, and contractions play an important role in reducing pressure losses. Research has been done throughout the years about how to choose a contraction ratio and wall design, as well as how to evaluate the performance of wind tunnels. The basic guidelines for developing a contraction portion are that it must produce a consistent and uniform stream and be able to withstand a particular amount of pressure. The contraction length must be as short as possible to avoid flow separation and provide as much relief as appropriate [11]. Non-uniformities at the exit plane must be handled with a minimum boundary layer thickness. for a given application, comparable to the highest level of tolerance (0.5 percent outside of the boundary layer). Although large contraction ratios are advantageous, they also imply higher development and operating expenses, and also the probability of noise and disconnection near the end. Before contraction, there is a settling chamber which is made using plastic straws and its purpose is to make the air move in a straight line. We used straws with a diameter of 0.5 cm and a length of 10 cm. Before exiting the wind tunnel, the air is channeled via a diffuser after reaching the test section. The diffuser, which increases the wind velocity in the test area, is the most important element of a wind tunnel. Inside the test tube, the diffuser creates a vacuum. As a result of the vacuum created inside the test tube wind velocity inside the restriction decreases and increases in the tube [12]. Different parts of the wind tunnel and our project's methodology are explained comprehensively in the next part of the paper.

2. Materials and Methods

2.1. Design of Wind Tunnel

An open return wind tunnel consists of three main components: Diffuser, test chamber, and contraction chamber. The overall design of an open return wind tunnel is shown in Fig. 1. Our main goal is to design a low-cost, low-speed wind tunnel that can be used as lab equipment in our university (for educational and research purposes). The main design criteria are to achieve a flow of (15-15 m/s), flow uniformity, and a low turbulence level inside the test chamber.

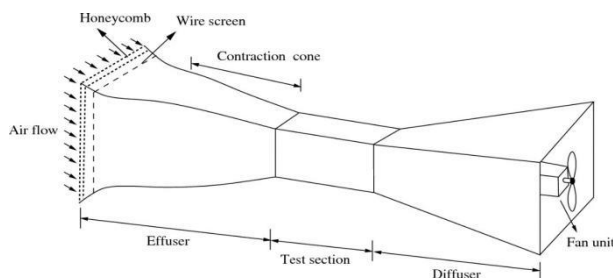


Figure 1. Wind tunnel parts and layout.

An essential aspect of wind tunnels is the quality of the flow within the test chamber. Therefore, creating a controlled

flow within the test chamber that satisfies the necessary standards for flow quality and productivity is the primary objective of wind tunnel design. Our wind tunnel design process was initially employed for the Spanish Consejo Superior de Deportes' theoretical LSWT, having a test section of $35 \times 35 \times 35 \text{ cm}^3$ and a maximum operating speed of 40 m/s. A similar approach is currently being used to create an LSWT for the University of Engineering & Technology, Jalozai campus. In a test section measuring $1.4 \times 1.0 \times 2.0 \text{ m}^3$, it will exhibit a high-quality flow rate of up to 10 m/s. It will be used for aerodynamic tests of aerofoil etc. The final design of the wind tunnel is shown in Fig. 2.

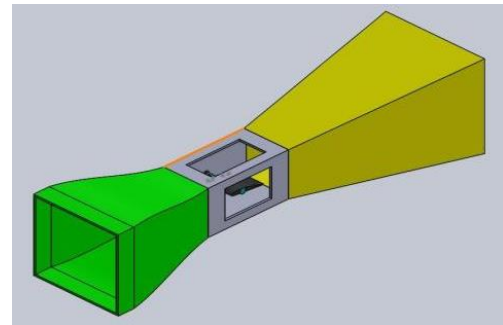


Figure 2. Final design of wind tunnel.

The author's low-speed wind tunnel is designed with emphasis on crucial parameters including size compactness, contraction angle, and diffuser length. This LSWT is distinguished by its mobility, which allows for easy construction and disassembly while maintaining precision in aerodynamic testing. The compact design allows for adaptation to a wide range of testing conditions without sacrificing precision, and the contraction angle has been carefully tuned to improve airflow pattern dependability and repeatability. The wind tunnel is user-friendly, as seen by its ease of installation and disassembly, making it an ideal tool for students and researchers to improve aerodynamic analysis efficiency. LSWT is a useful instrument for conducting detailed aerodynamic tests. Its ability to compute drag and lift provides another layer of capability, allowing researchers to dive into the complexities of aerodynamic forces. As the need for advanced aerodynamic testing grows, the author's low-speed wind tunnel emerges as a critical tool, combining flexibility, accuracy, and analytical capabilities to drive advances in aerodynamic research and engineering innovation.

2.2. Dimensions

Contraction Chamber: Length = 105.85 cm, Initial Height = 75.00 cm, Final Height = 30.00 cm, Contraction Angle = 12°

Test Chamber: Length = 1.00 m, Height and Width = 30 cm

Diffuser Dimensions: Length = 228.601 cm, Initial Height = 30.00 cm, Final Height = 70.00 cm, Expansion angle = 5°

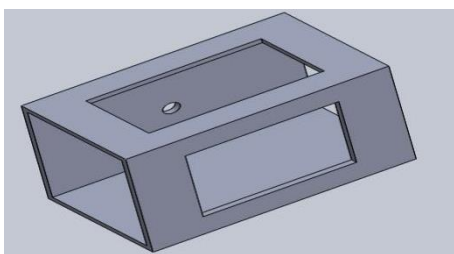
Table 1 shows the details of the material used for the low-speed wind tunnel.

Table 1 Material details of low-speed wind tunnel.

Name	Assigned to	Properties	
ABS (Molde)	Airfoil	X-Direction	0.153 W/m-K
		Y-Direction	0.153 W/m-K
		Z-Direction	0.153 W/m-K
		Density	1.05 g/cm ³
		Specific heat	2.05 J/g-K
		Emissivity	0.469
		Transmissivity	0.0
		Electrical resistivity	165000000000000.00
		Wall roughness	0.0 meter
Air	Environment fluid	Density	Equation of State
		Viscosity	1.817e-05 Pa-s
		Conductivity	0.02563 W/m-K
		Specific heat	1004.0 J/kg-K
		Compressibility	1.4
		Emissivity	1.0
		Wall roughness	0.0 meter
		Phase	Vapor Pressure

2.3. Test Chamber

Between the diffuser and the region of contraction is the test section. Since the test section is the area where readings and analysis are done, a thorough layout of the test chamber is required. The test chamber must be large enough to adequately dampen flow disturbances caused by the contraction cone before they reach the object. The size and form of the test portion are both critical. In our case, a rectangular shape (which is easy to produce) is appropriate and suggested for aviation purposes. The standard width/height ratio in a three-dimensional test is 4:3. Moreover, the cavity of the test chamber should be smooth and well-sealed so that airflow is laminar and no air leakage from the test chamber. The detailed CAD model of the test section is shown in Fig. 3, Fig. 4, and Fig. 5.

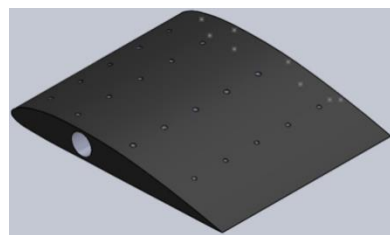
**Figure 3.** SolidWorks model of test section.

2.4. Airfoil and Load Cell Arrangement

After the test chamber model, we now want to make a CAD model of an airfoil. So that we can use it inside the test chamber to test its aerodynamic properties i.e., to find the lift and drag force acting on it, using load cell arrangement.

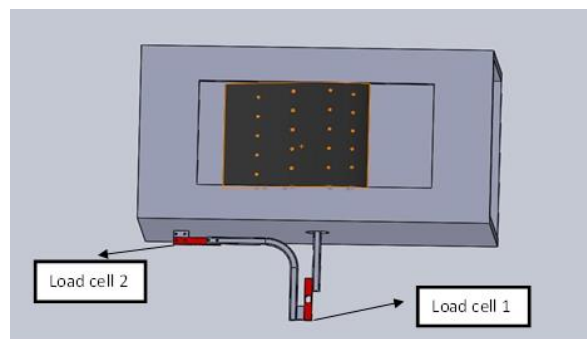
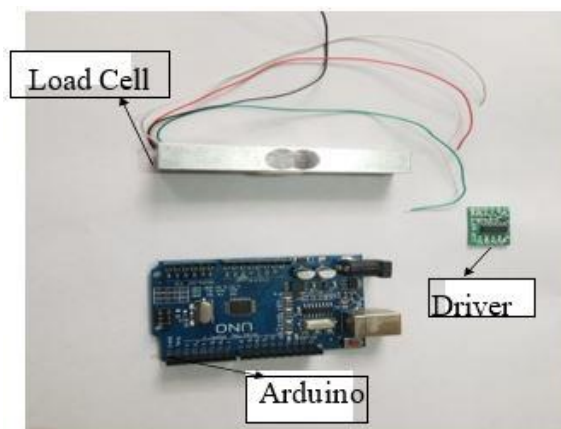
An aerofoil, often known as an airfoil, is a wing, tail, or propeller blade with a curved surface that, when moved through the air, creates lift and drag. The lifting force of an airfoil is perpendicular to the direction of the airstream,

whereas the dragging force is perpendicular to it. The CAD model of our airfoil (Clark-y airfoil) is shown in Fig. 4.

**Figure 4.** Y-Clark airfoil designed in SolidWorks.

2.5. What is a Load Cell?

One way to measure force is with a load cell. It converts a non-measurable force, such as a moment, compressive force, stress, or tensile force, into an electrical signal with precise measurements. A load cell's electrical output is proportional to the force applied to it. The three most common kinds of load cells are strain gauges, hydraulic load cells, and pneumatic load cells. Fig. 5 and Fig. 6 show how the load cells are arranged with the airfoil.

**Figure 5.** Load cells arrangement with airfoil.**Figure 6.** Load cells installed on wind tunnel.

In our case, we used electric strain gauge-type load cells which were connected to Arduino UNO (microcontroller). We used two load cells one will measure drag force and the other will be used to measure the lift force acting on the airfoil.

2.6. Contraction Chamber

Air first enters the contraction chamber and then flows into the test section. The contraction chamber leads to a compression of air due to which the velocity of the air entering the test chamber increases. The rate of turbulence decay can be adjusted by the contraction area. Airflow through the contraction cone modifies turbulence by lowering shifting velocity variations and reduces turbulence levels. Therefore, the contraction chamber needs to be meticulously designed. The ratio is the most critical variable to consider while constructing the contraction cone. Most tiny subsonic wind tunnels have a contraction ratio between 6 and 10.

To achieve these objectives a settling chamber is used. It will be placed at the very beginning of the wind tunnel i.e. at the start of the contraction chamber. A honeycomb structure will be present inside the settling chamber to maintain uniform air velocity inside the wind tunnel. Making the honeycomb structure was a tedious job. The honeycomb component of this project was constructed by cutting and assembling dozens of wall panels. The length of the wall panels was 10 cm and inner diameters were 0.9 cm, outer diameters were 1 cm. We joined these wall panels together with the help of silicon glue. These bonds were strong enough to sustain a high velocity of wind. This honeycomb arrangement may transform turbulent winds into a uniform flow that reaches the contraction area. Our settling chamber along with the honeycomb structure is shown in Fig. 7. The CAD model of the contraction chamber is shown in Fig. 8.



Figure 7. Settling chamber of wind tunnel.

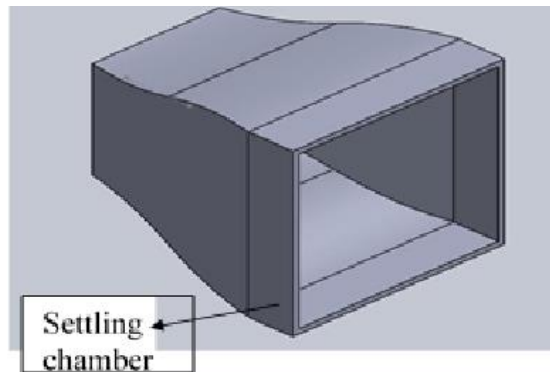


Figure 8. SolidWorks model of contraction chamber.

2.7. Diffuser

The diffuser is an essential component of a wind tunnel. and careful design of the diffuser is necessary. The wind tunnel's diffuser sits just before the fan and is the final component. Instead of using a blower, the fan draws air into the wind tunnel, which makes the test area less turbulent.

A bigger diffuser cross-section area causes the air entering it from the test section to expand, which in turn causes the velocity to drop. Thus, it creates a vacuum in the test section leading to a decreased restriction and increased velocity of wind inside the test section [13].

3. Fabrication of Wind Tunnel

Now that our design is ready it's time for fabrication. We used an MDF board (Medium-density fibreboard). to construct the wind tunnel. It's an engineering material manufactured by disintegrating hardwood and softwood into wood fibers, usually in a defibrator, mixing it with paraffin and a resin binder, and shaping it into panels using high heat and pressure. Compared to plywood, MDF is denser. Its composition of fragmented fibers belies its usefulness as a chipboard-like building material. It outperforms particle board in terms of density and strength. We have used the MDF board due to its greater strength and density than normal wooden boards. It has a low cost, and it is also easy to fabricate as compared to sheet metal. Each part of the wind tunnel (contraction chamber, test chamber, diffuser) was fabricated using an MDF board with the help of nails and epoxy. Epoxy was used to prevent the leakage of air. Contraction chamber fabrication is shown in Fig. 9. The test chamber made in our project is shown in Fig. 10.



Figure 9. Contraction chamber.

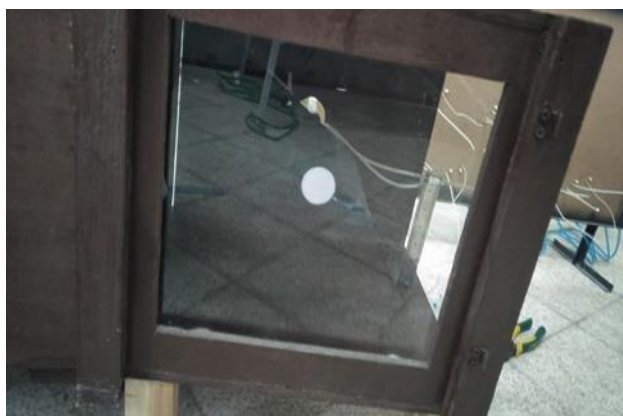


Figure 10. Test chamber.

3.1. 3D Printed Airfoil

The 3D-printed airfoil model along with the shaft is shown in Fig. 11. It is made up of plastic material. A Pitot tube with an airfoil is shown in Fig. 12.



Figure 11. 3D printed airfoil.



Figure 12. Pitot tube and airfoil in wind tunnel.

3.2. Manometer

Manometers are used to measure small pressure differences. We used an inclined plane manometer to measure pressure at different points of airfoil. This manometer consists of 10 tubes, inclined at an angle of 30 degrees, (1 unit along the vertical axis will show 2 units readings at 30 degrees). Two tubes are connected to the pitot tube to measure static and stagnation pressure while eight tubes are connected to the

airfoil, to study pressure variations along the airfoil. Each tube has a diameter of 5 mm and length of 62 cm and is filled with water up to a specific point. The inclined tube manometer used is shown in Fig. 13.

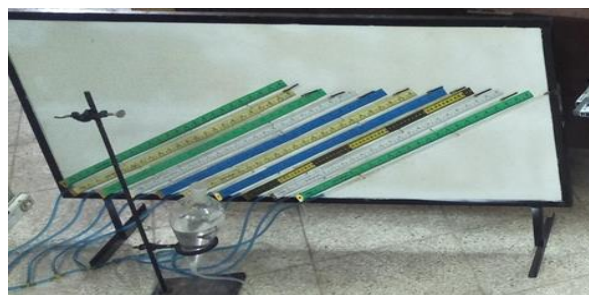


Figure 13. Inclined tubes manometer.

3.3. Wind Tunnel Assembly

The assembly of our fabricated project is shown in Fig. 14 and Fig. 15.



Figure 14. Wind tunnel assembly.



Figure 15. Assembly of fabricated parts of wind tunnel.

4. CFD Analysis

We used Fusion 360 a CAD software for simulations [14]. In the test section of the wind tunnel, calculations of airfoils are carried out. All the relevant data and results obtained from the CFD analysis are described in this section.

4.1. Design

The design of the airfoil is shown in Fig. 16.

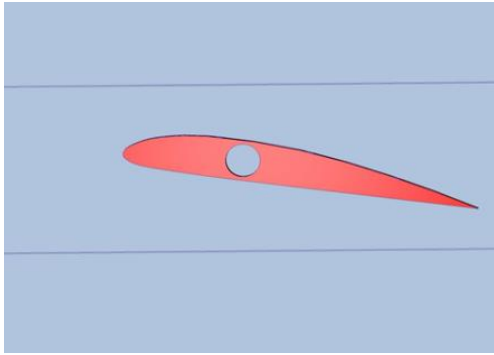


Figure 16. Airfoil design.

4.2. Boundary Conditions

Table 2 outlines the boundary conditions that were specified in the CFD Analysis at the inlet and outlet.

Table 2. Boundary condition.

Type	Assigned to
Pressure (1 atm Gage)	outlet
Velocity Normal (20 m/s)	inlet

4.3. Automatic Meshing Settings

Table 3 and Table 4 show the automatic mesh setting and mesh refinement setting for the low-speed wind tunnel that was used in the analysis.

Table 3. Automatic mesh setting.

Surface refinement	0
Gap refinement	0
Resolution factor	1.0
Edge growth rate	1.1
Minimum points on the edge	2
Points on the longest edge	10
Surface limiting aspect ratio	20

4.4. Mesh Enhancement Settings

Mesh details of the airfoil section are shown in Fig. 17.

Table 4. Mesh enhancement setting.

Mesh enhancement	1
Enhancement blending	0
Number of layers	3
Layer factor	0.45
Layer gradation	1.05

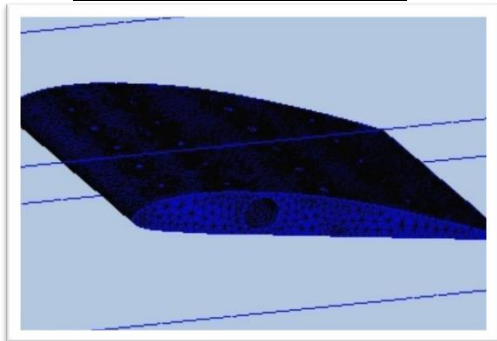


Figure 17. Meshed model airfoil.

4.5. Solver Settings

The solver setting for CFD Analysis is shown in Table 5.

Table 5. Solver settings.

Solution mode	Steady State
Solver computer	My computer
Intelligent solution control	On
Advection scheme	ADV 5
Turbulence model	k-epsilon

4.6. Mass Balance

Mass Balances At the inlet and outlet are shown in Table 6.

Table 6. Mass balance.

	In	Out
Mass flow	640.818 g/s	639.099 g/s
Volume flow	531916.0 cm ³ /s	530489.0 cm ³ /s

4.7. Pressure Contour

The pressure contours of the airfoil section at different angles are shown in Fig. 18 and Fig. 20. Velocity contours at 25° and 10° are shown in Fig. 19 and Fig. 21.

Pressure profile at 25 degrees

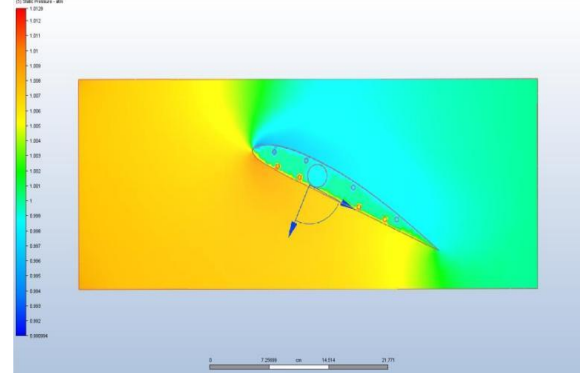


Figure 18. Pressure profile at 25 degrees.

Velocity profile at 25 degrees

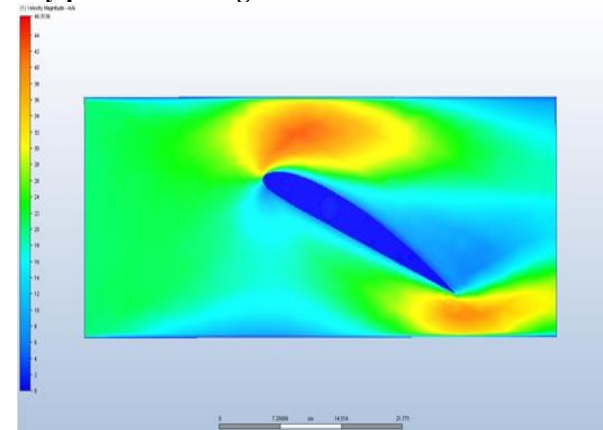


Figure 19. Velocity profile at 25 degrees.

Pressure profile at 10 degrees

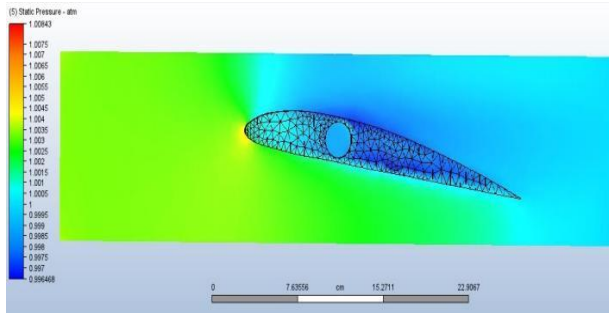


Figure 20. Pressure profile at 10 degrees.

Velocity profile at 10 degrees

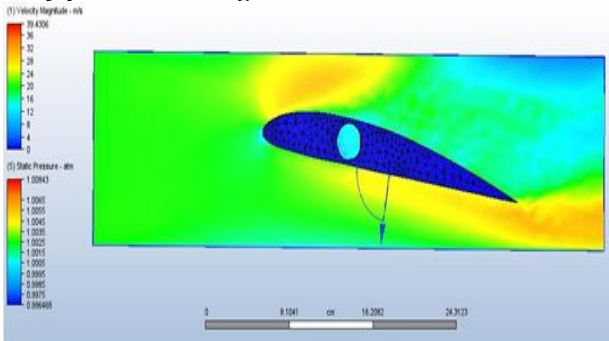


Figure 21. Velocity profile at 10 degrees.

5. Data Acquisition & Processing

The system to obtain data is made up of two load cells with their respective amplifiers (Hx7110, which is a 24-bit precision analog to digital converter and amplifier), connected to Arduino. Also, the program (code) is saved in Arduino, power is provided to Arduino with a charger, and the display screen shows the value of lift and drag measured by the load cells in Newton and grams. The code is displayed in [Appendix A](#). The maximum range of each load cell is 49 N. The connections of the load cell with Arduino, driver, and display screen are shown in [Fig. 22](#).

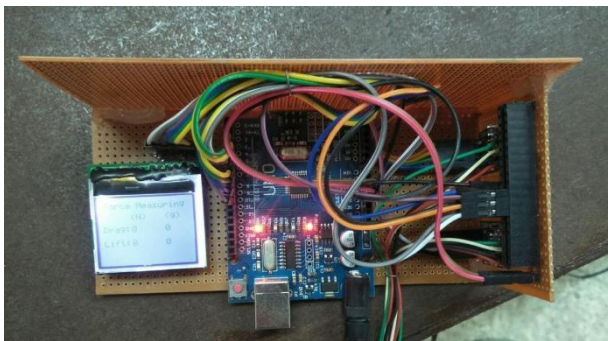


Figure 22. Connection of load cells with Arduino, driver, and display screen.

6. Results and Discussion

6.1. Calculating the Velocity of Air

Calculating the velocity of air in the wind tunnel is the first step toward finding the aerodynamics of the airfoil in the

wind tunnel. The velocity of air in the wind tunnel is also needed to find the Reynolds number of the airfoil, which tells us about the behavior of fluid around the airfoil, whether it is laminar or turbulent [15].

Different techniques are used to find the velocity of air in the wind tunnel, which includes the pitot tube and inclined tube manometer. Pitot static tubes determine fluid velocity by evaluating stagnation pressure, which is equal to the total of static and dynamic pressure. Two tubes came out from the pitot tube, one was for stagnation pressure also called total pressure, other was for static pressure. These tubes are connected to the upper ends of tubes of the manometer, which is filled with water up to a specified scale. By applying Bernoulli's Equation [16], we get the expression of velocity as: -

$$= \frac{\sqrt{2(P_2 - P_1)}}{\rho} \quad (1)$$

Also, $P_2 = \rho g h_2$ (Total /Stagnation pressure)

$P_1 = \rho g h_1$ (Static Pressure)

So, we get the expression for velocity as:

$$= \sqrt{2g(h_2 - h_1)} \quad (2)$$

Here, $h_2 - h_1$ is the change in the head (difference between the static head from the dynamic head), it is noted, and by putting it in the equation we get the velocity of air in the wind tunnel.

We can also find the velocity of air in the wind tunnel, from the flow rate formula which is given by.

$$Q = Av \quad (3)$$

Here, Q= Air flow rate

A = frontal area of the test chamber

V = Velocity of air in the wind tunnel/ test section

Also, we know that,

Q= 2500 cfm (cubic feet per minute)

$$= 1.168 \text{ m}^3/\text{sec}$$

$$A = 35 \text{ cm} \times 35 \text{ cm}$$

$$= 0.1225 \text{ m}^2$$

Hence, we can find the velocity of air as

$$Q = Av$$

$$v = \frac{Q}{A} = \frac{1.168 \text{ m}^3/\text{sec}}{0.1225 \text{ m}^2} v = 9.53 \text{ m/sec}$$

6.1.1. Reynolds Number for Airfoil

We can find the Reynolds Number for airfoil from the following formula [17].

$$Re = \frac{\rho v L}{\mu} \quad (4)$$

Here ρ = Density of air =, L = average length, v = flow velocity in our case of airfoil it is equal to the length of the airfoil, which is 25 cm, and μ = dynamic viscosity.

Also, $\rho = 1.25 \text{ kg/m}^3$, $v = 9.5 \text{ m/sec}$, $L = 0.25$, $m = 1.85 \times 10^{-5} \text{ kg/m.sec}$.

Now

$$Re = \frac{\rho v L}{\mu} Re = \frac{(1.225 \text{ kg/m}^3)(9.5 \text{ m/sec})(0.25 \text{ m})}{1.85 \times 10^{-5} \text{ kg/m.sec}}$$

$$Re = 1.572 \times 10^5$$

First of all, we take the value of load cells for lift and drag, from the display screen which is placed next to Arduino. After that, we calculate the coefficients of drag and lift, and we compare the values of drag and lift upstream velocity. Now the values of all the above parameters are given below for standard atmospheric temperature and pressure conditions: The lift force for the 0° angle of attack is found to be 0.2940 N. The drag force for the 0° angle of attack is found to be 0.1176 N.

6.2. Calculating Lift and Drag Coefficients

Now we will find the lift and drag coefficient i.e. C_L and C_D .

6.2.1. Find the Coefficient of Lift for 0 Degrees AOA

The formula for the Coefficient of lift is as follows:

$$C_L = \frac{F_L}{\frac{1}{2} \rho V^2 A} \quad (5)$$

Lift Force is 0.2940 N. The density of Air is 1.225 kg/m^3 . The velocity is 9.5 ms^{-1} . The frontal Area of the Airfoil is 0.05 m^2 .

$$C_L = \frac{0.2940 \text{ N}}{\frac{1}{2} (1.225 \text{ kg/m}^3) (9.5 \text{ m/s})^2 (0.05 \text{ m}^2)}$$

$$C_L = 0.1063$$

So, the Lift Coefficient is determined to be 0.1063 for the Y-Clerk airfoil at 0° AOA.

6.2.2. Finding Coefficient of Drag for 0 Degree AOA

The formula for the Coefficient of Drag is as follows:

$$C_D = \frac{F_D}{\frac{1}{2} \rho V^2 A} \quad (6)$$

where C_D is the drag coefficient, F is the drag force, ρ is the air density, V is upstream flow velocity and A is the frontal area of the airfoil.

Now the values of all the above parameters are given below for standard atmospheric temperature and pressure conditions: The Drag Force is 0.1176 N. The density of Air is 1.225 kg/m^3 . The velocity is 9.5 ms^{-1} . The frontal area of the airfoil is $25 \text{ cm} \times 5 \text{ cm} = 0.01 \text{ m}^2$.

$$C_D = \frac{0.1176 \text{ N}}{\frac{1}{2} (1.225 \text{ kg/m}^3) (9.5 \text{ m/s})^2 (0.01 \text{ m}^2)}$$

$$C_D = 0.2127$$

So, the Lift Coefficient is determined to be 0.2127 for the Y-Clerk airfoil at 0° AOA angle of attack. Doing similar calculations for all angles of attacks, from 0° to 60° , For the measurements of lift and drag forces, and coefficient of lift and drag, we got the following Table 7.

Table 7. Lift and drag at AOA (0 TO 60) degrees.

Angle of Attack	Drag Force	Lift Force	Drag Coefficient	Lift Coefficient
0	0.1176	0.294	0.2127	0.1063
10	0.1576	0.784	0.3284	0.2836
20	0.452	1.0486	0.4568	0.3793
25	0.650	1.274	0.5520	0.4609
30	0.850	1.176	0.6150	0.4254
40	1.550	1.078	0.8727	0.39
50	2.310	0.98	1.0910	0.3545
60	3.52	0.833	1.4706	0.3013

Lift and Drag increase with the increase in the angle of attack of an airfoil, up to A stall is developed whenever the angle of attack of an airfoil is above the value that produces optimum lift as a result of flow across it, we can see from the table that, the maximum lift force occurs at 25° and its magnitude is 1.274 N. Also, if we increase the angle of attack beyond 25° , lift force will decrease, and stall will occur at 25° . Also, it is noted that the frontal area of the airfoil changes with a change in the angle of attack.

At 0° AOA, the frontal area of the airfoil is:

$$\text{Area} = \text{width} \times \text{thickness} = 20 \text{ cm} \times 5 \text{ cm} = 0.01 \text{ m}^2$$

Similarly, at Angle of Attack θ , find the frontal area of the airfoil by using the formula.

$$\text{Frontal Area} = \text{Width} \times \text{Lenth} (\sin \theta) \quad (7)$$

We get the following values for the angle of attack from 10 to 60 degrees. Table 8 gives the area of the airfoil at different angles of attack.

Table 8. Frontal area of airfoil at different angles of attacks.

Area	Angle of Attack
0.01	0
0.00868	10
0.0179	20
0.0213	25
0.025	30
0.03213	40
0.0383	50
0.0433	60

Similarly, the graphs are also shown below for this data.

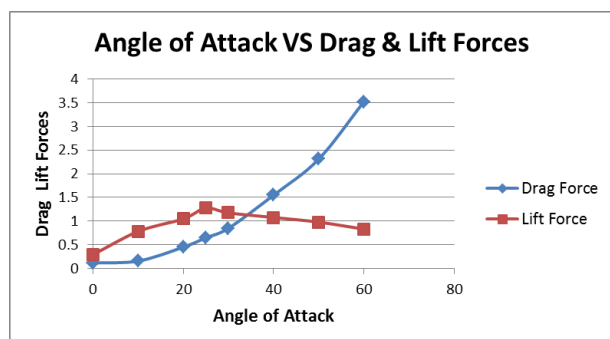


Figure 23. Combine graph of angle of attack vs drag & lift forces.

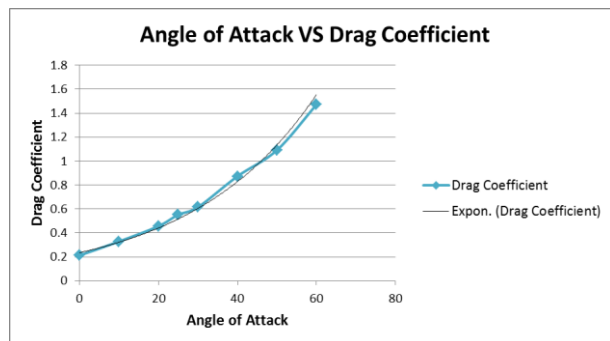


Figure 24. Graph of angle of attack vs drag coefficient.

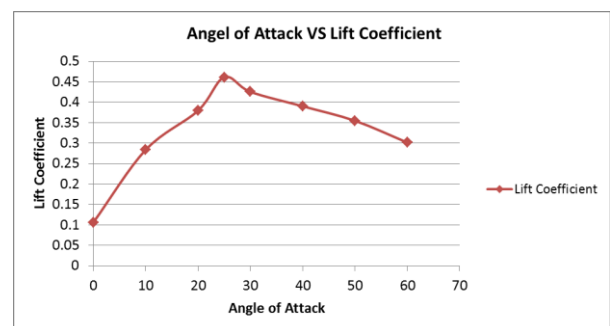


Figure 25. Graph of angle of attack vs lift coefficient.

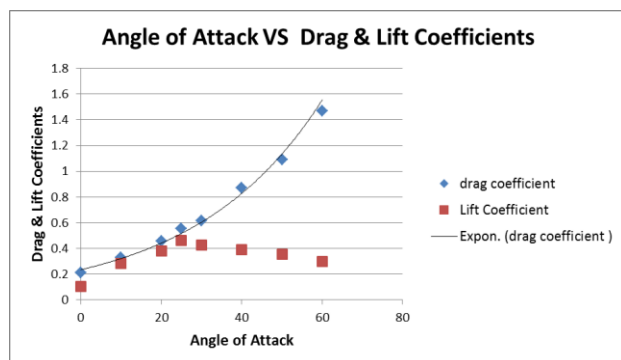


Figure 26. Combine graph of angle of attack vs lift & drag coefficients.

We have discussed that the coefficients of lift and coefficient of drag increase with increasing the angle of attack, hence it is clear from Fig. 23, Fig. 24, and Fig. 25. Also from Fig. 25, it is seen that the maximum lift coefficient occurs at 25° with a magnitude of 0.4609 and the maximum

drag coefficient occurs at 60° with a magnitude of 1.4706. The relation between the angle of attack and drag and lift forces is illustrated 0.4609 and the relation with drag coefficient is shown in Fig. 26.

7. Conclusions

This study outlines a rapid low-speed wind tunnel design method executed using SolidWorks and constructed using a medium-density fiber (MDF) board. The main purpose was to examine the aerodynamics of the Y-Clerk Airfoil. Load cells and Arduino were used to measure the lift and drag forces across varying angles of attack, subsequently generating drag and lift coefficients. Wind tunnel air velocity and airfoil pressure were assessed using an inclined tube manometer and a pitot tube, respectively. Experiments were conducted at different angles of attack after fabrication and installation, revealing the following key findings:

- Lift and drag forces are proportional to the angle of attack until stall, with the highest coefficient of lift occurring at 25 degrees.
- The highest lift coefficient is 0.4609.
- The wind speed within the tunnel is 9.5 m/s, and the stall takes place at a 25-degree angle of attack.

Enhancements to optimize wind tunnel performance are recommended:

- Use high-quality materials for the contraction and diffuser sections to optimize flow airflow quality, profile smoothness, and pressure loss reduction.
- Employ a potent motor with an axial fan, considering a multi-fan mechanism to augment air velocity.
- Add a damper system to counteract fan-induced vibrations.
- Install a smoke generator to see the airflow over the airfoil.
- The ultimate recommendation is to build a new table or platform for the wind tunnel structure to increase its stability and functionality.

List of Abbreviations

LSWT	Low-speed Wind Tunnel
CFD	Computational Fluid Dynamics
CAD	Computer Aided Drawing
MDF	Medium Density Drawing
AOA	Angle of Attack

Availability of Data and Materials: All the relevant data will be shared upon request by the corresponding author.

Competing Interests: The authors declare no conflict of interest.

Funding: No funding was attained for this project.

Authors Contributions: UA (Umair Asghar) contributed to the conception of the study. MAW (M. Anas Wazir) and Muhammad Kaleem Wazir (MKW) organized the database. Abbas Khan, Muhammad Usama and Osama Subhan (OS) performed the experimental analysis. MAW and UA wrote the first draft of the manuscript. All authors contributed to the fabrication process of the project. All authors contributed to the manuscript revision and approved the final submitted version of the manuscript.

Acknowledgments: The authors acknowledge the support of UET Peshawar for providing the computational facilities to conduct this research.

Appendix A

Arduino Programing for Load Cells: The vertical load cell provides the measurement of the lift force generated on the airfoil, while the horizontal load cell provides the value of the drag force generated on the airfoil. The program used to obtain the readings from the load cells is as follows:

```
#include "HX711.h"
#include "Megatronics_pk_lcd.h"
Megatronics_pk_lcd lcd(10, 9, 7, 8); // RST, MISO, MOSI,
SCK, or you can change to any pin.
const int LOADCELL_DOUT_PIN = 3; const int
LOADCELL_SCK_PIN = 4; const int
LOADCELL_DOUT_PIN1 = 5; const int
LOADCELL_SCK_PIN1 = 6;
float val, val2, tar=0.0, tar2=0.0, val_g=0.0, val_g2=0.0; int
button=2;
```

```
HX711 scale;
void setup() { Serial.begin(9600);
pinMode(button, INPUT_PULLUP); lcd.Begin();
lcd.Clear_LCD();
}
void loop() {
scale.begin(LOADCELL_DOUT_PIN,
LOADCELL_SCK_PIN);
val= ((scale.get_units(5))/460)*0.0098; if(digitalRead(button)
== LOW){ tar=val;}[15] val_g=(val-tar)/0.0098;
lcd.print(2, 1, 1, "Force Measuring");
lcd.print(31, 14, 1, "(N)"); lcd.print(69, 14, 1, "(g)");
lcd.print(1, 28, 1, "Drag:");
lcd.print(32, 28, 1, val-tar);
lcd.print(69, 28, 1, val_g);
```

```
scale.begin(LOADCELL_DOUT_PIN1,
LOADCELL_SCK_PIN1);
val2= ((scale.get_units(5))/460)*0.0098;
if(digitalRead(button) == LOW){ tar2=val2;} val_g2=(val2-
tar2)/0.0098;
lcd.print(1, 44, 1, "Lift:");
lcd.print(32, 44, 1, val2-tar2);
lcd.print(69, 44, 1, val_g2); lcd.Update(); lcd.Clear_LCD();
}
```

References

- [1] J. D. Anderson, *A History of Aerodynamics: And Its Impact on Flying Machines*. Cambridge University Press, 1998.
- [2] J. B. Barlow, W. H. Rae, and A. Pope, *Low-Speed Wind Tunnel Testing*. Wiley, 1999.
- [3] R. Howell, N. Qin, J. Edwards, and N. Durrani, "Wind Tunnel and Numerical Study of a Small Vertical Axis Wind Turbine," *Renewable Energy*, vol. 35, pp. 412-422, 02/01 2010.
- [4] N. Maurya, M. Manish, A. Tyagi, and S. Dwivedi, "Design & Fabrication of Low-Speed Wind Tunnel and Flow Analysis," *International Journal of Engineering and Technology (UAE)*, pp. 381-387, 12/01 2018.

- [5] A. A. Kareem, M. K. Abbas, and F. A. Khammas, "Aerodynamic Study of Low-Speed Wind Tunnel Contraction Section: Design and Manufacturing," *IOP Conference Series: Materials Science and Engineering*, vol. 1094, no. 1, p. 012077, 2021/02/01 2021.
- [6] A. Patil and K. Kulkarni, "Design and Fabrication of Low-Speed Wind Tunnel," *SMART MOVES JOURNAL IJOSCIENCE*, pp. 11-19, 04/28 2021.
- [7] R. A. Siregar and K. Umurani, "Laboratory development of low-speed wind tunnel for educational purposes," *IOP Conference Series: Materials Science and Engineering*, vol. 670, no. 1, p. 012059, 2019/11/01 2019.
- [8] J. Farnsworth, D. Sinner, D. Gloutak, L. Droste, and D. Bateman, "Design and qualification of an unsteady low-speed wind tunnel with an upstream louver system," *Experiments in Fluids*, vol. 61, no. 8, p. 181, 2020/07/28 2020.
- [9] R. Kubesh and B. Allie, "A Wind Tunnel for an Undergraduate Laboratory," *International Journal of Mechanical Engineering Education*, vol. 37, pp. 21-26, 01/01 2009.
- [10] B. Chanetz, "A century of wind tunnels since Eiffel," *Comptes Rendus Mécanique*, vol. 345, no. 8, pp. 581-594, 2017/08/01/ 2017.
- [11] R. D. Mehta and P. H. Hoffmann, "Boundary layer two-dimensionality in wind tunnels," *Experiments in Fluids*, vol. 5, no. 5, pp. 358-358, 1987/09/01 1987.
- [12] J. Roskam and C. T. E. Lan, *Airplane Aerodynamics and Performance*. Roskam Aviation and Engineering, 1997.
- [13] S. S. Abdel Aziz, E. B. Moustafa, and A.-H. S. Salem Said, "Experimental Investigation of the Flow, Noise, and Vibration Effect on the Construction and Design of Low-Speed Wind Tunnel Structure," vol. 11, no. 3, p. 360, 2023.
- [14] L. Leifsson, S. Koziel, F. Andrason, K. Magnusson, and A. Gylfason, "Numerical Optimization and Experimental Validation of a Low-Speed Wind Tunnel Contraction," *Procedia Computer Science*, vol. 9, pp. 822-831, 2012/01/01/ 2012.
- [15] M. Biazewicz, K. Kurowski, B. Ludwiczak, and K. Napierała, "Problems Related to Parallelization of CFD Algorithms on GPU, Multi-GPU and Hybrid Architectures," in *Icnaam 2010: International Conference of Numerical Analysis and Applied Mathematics 2010*, 2010, vol. 1281, pp. 1301-1304.
- [16] N. A. a. S. Administration, *Bernoulli Equation*. Available: <https://www.grc.nasa.gov/www/k-12/airplane/bern.html>
- [17] E. Krause, *Fluid Mechanics: With Problems and Solutions, and an Aerodynamics Laboratory*. Springer, 2005.